*Proceedings of the*
*Annual Stability Conference*
*Structural Stability Research Council*
*San Antonio, Texas, March 19-22, 2024*

# Pilot Research on Long-Span Cold-Formed Steel Trusses

Sai Kumar. Nalla[1], Cheng. Yu, PhD, PE[2]

## Abstract

To meet the increasing demand for long-span (50+ ft) cold-formed steel trusses, a pilot research program was recently conducted in the structural testing lab at the University of North Texas. The research took advantage of recent cold-formed steel fabricating technologies by using innovative member configurations in the truss members' design. The research was also aimed at improving the cost effectiveness and fabrication easiness of the overall trusses by adopting a single member profile for the entire truss. The paper focused on the different failure modes and developed improvement methods during the research program. The pilot research indicated that light-gauge cold-formed steel members could be used in fabricating long-span trusses with special design attention in connections and joints.

## 1. Introduction

In the construction industry, steel plays a pivotal role, with two main types: cold-formed steel (CFS), shaped at room temperature, and hot-formed steel, heated and rolled. CFS offers advantages such as material uniformity, durability, strength, and low weight, making it increasingly popular in modern construction. Common CFS shapes, including C-sections, Z-sections, angles, hat sections, tubular members, etc., find applications in structural framing, non-structural framing, decking, panels, and bridge forms. Trusses, an engineering framework comprising triangle-shaped components, distribute loads effectively, with steel trusses being preferred for their strength and durability, especially in bridge construction. Trusses, whether made of concrete, steel, or wood, are versatile and cater to specific use cases. Various types of trusses, such as King Post, Queen Post, Pratt, Howe, and Square End, offer strength and lightweight characteristics, making them suitable for diverse applications like building floors and roofs in the construction field.

Trusses made of cold-formed steel members are limited in the overall span due to insufficient stability of individual elements and large flexibility of the overall structural assembly. However there has been a strong demand for long-span cold-formed steel trusses due to its excellent attributes of quick production, easy transportation, and overall high cost-effectiveness.

---

[1] Graduate Research Assistant, University of North Texas, <Saikumarnalla@My.UNT.edu>
[2] Professor, University of North Texas, <Cheng.Yu@UNT.edu>

This paper presents a pilot research effort to address an increasing demand for a non-proprietary, easily built, long-span truss using AISI standard CFS sections. The specific features of the new truss design are:

1. One single AISI standard CFS member is used for the entire truss structure;
2. Screws connections;
3. Span over 48 ft.;
4. Reduced truss depth.

## 2. Desing concept

Fig. 1 shows the concept of the proposed novel long-span CFS truss. The truss is constructed using one single stud section profile. To reinforce the top and bottom chords, modified back-to-back composite CFS sections were used. For the top chords, two layers of back-to-back sections were designed as high compression forces are expected. For the bottom chords, a single back-to-back section is adopted, and it could be further reinforced by additional layers. To enhance the composite behavior, additional CFS sections were used on the exterior flanges of the chords. For the web members, various configurations were investigated in this project. Fig. 1 shows the initial concept which utilized a single CFS section. The web section is coped at both ends to allow a secure connection to the chords. Fig. 1 also illustrates the screw locations in the chords to ensure a composite behavior in the assembled members. It is worth mentioning that this was a pilot research project, the truss configuration had been continuously improved and changed during the testing and Finite Element Analysis (FEA) processes.

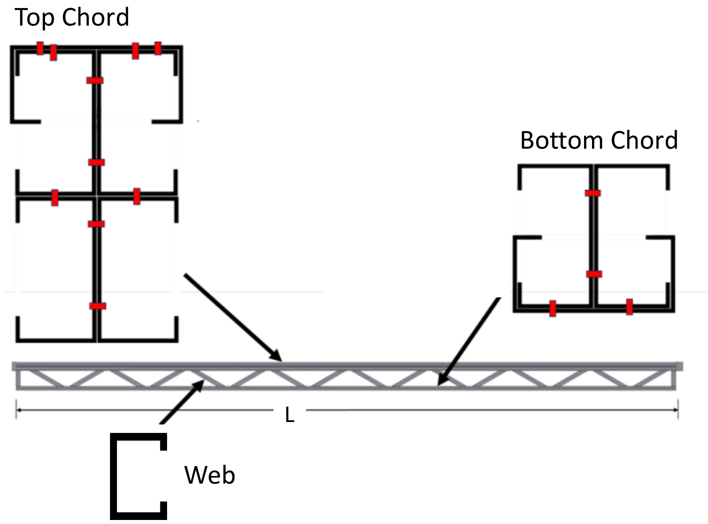

Figure 1: Concept of the Proposed Novel Long-Span CFS Truss

## 3. Experimental study

### *3.1 Testing Setup*

Reported in the paper were static tests on four trusses. The truss tests were conducted in the Structural Testing Lab at the University of North Texas (UNT). Fig. 2 shows the overall truss testing frame at UNT. The truss is simply supported at both ends of the top chord. To apply uniform loads on the top chord of the truss a series of hydraulic cylinders used via load beams. The cylinders are placed 2 ft apart. A series of CFS cap members were used to connect the top chord to the load spread beam in order to restrict the out-of-plane movement of the top chord.

To measure the reaction force of the truss, a load cell is used at one support as shown in Fig. 3(b) since the truss is symmetric and the reaction force is assumed to be equal between the two supports. The vertical deflection of the center point of the bottom chord was measured by a position transducer as shown in Fig. 3(a). A series of wood plates are used to restrict the out-of-plane displacement of the bottom chord as shown in Fig. 2. The wood plates were placed 2 ft on center.

The truss tests were conducted using a force control method. The uniform load was continuously applied to the specimen until failure.

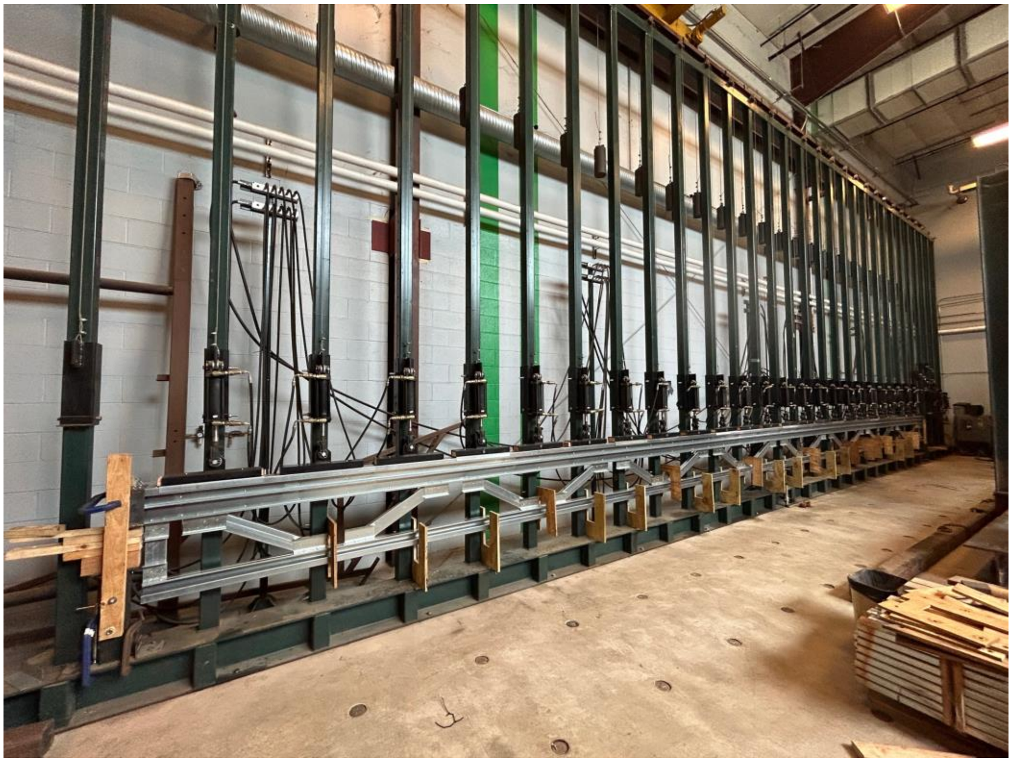

Figure 2: Truss Testing Frame at University of North Texas

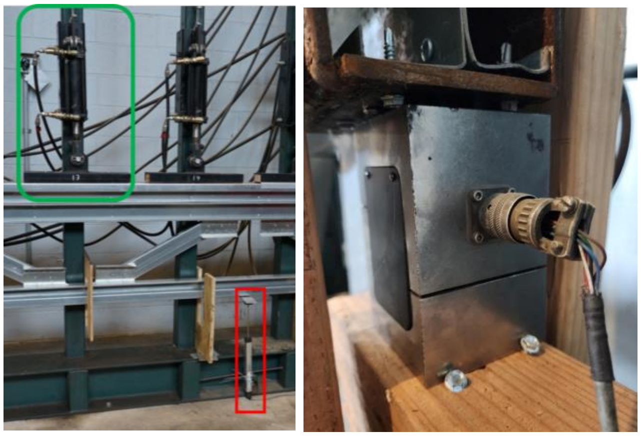

Figure 3: a) Deflection Sensor and CFS Member Cap to the Load Spread Beam; b) Load Cell at One Support

### *3.2 Truss Specimen Configurations*

The tested trusses had two spans: 48 ft and 54 ft. Two trusses in each span. All the trusses used the same CFS section: 362S162-43 with a yield stress of 50 ksi. Fig. 4 shows the profiles of the two span trusses.

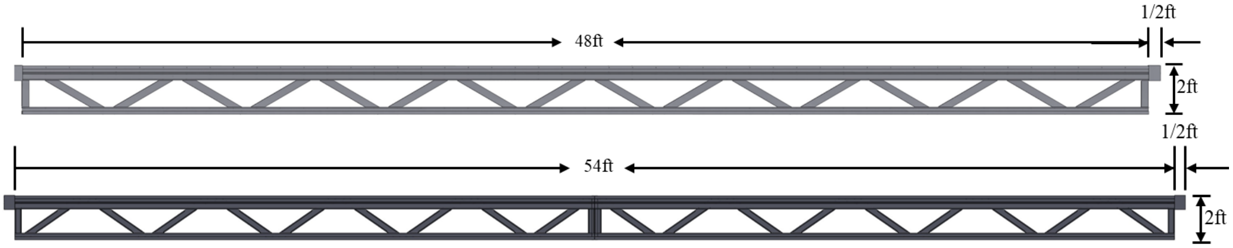

Figure 4: Profile of the Long-Span Trusses Tested at UNT

The 48 ft long trusses were constructed with continuous members for the chords. The 54 ft trusses were formed by assembling two 27 ft long trusses.

### *3.3 Reinforcement of the Webs*

The project team discovered that the web-to-chord connections needed reinforcement to avoid premature failure of the truss. Trusses have weak points at the connections of the webs with the top and bottom chords because there are no flanges and lips at the connections of the members. To overcome the weakness, we developed a few configurations to reinforce those weak points.

### *3.3.1 Clip Angle Type of Reinforcement*

In the first test we used the 350T162-54 member with No. 10 screws as a clip angle to reinforce the truss at weak points as shown in Fig. 5(a). The reinforcing track member was screwed to the chord and the web member. Fig. 5(b) shows the failure mode in the reinforcing member where a tension force was applied to the member and screw pull-out failures was observed. Failures in the web members were also observed in the first test.

Figure 5: a) Clip Angle Type of Reinforcement, b) Failure of the Reinforcing Member

### *3.3.2 Vertical Web Member Type of Reinforcement I*

After observing the first test's results, we found that the reinforcement at the weak points was not sufficient. Therefore, we added the vertical members at those web-to-chord joints as shown in Fig. 6(a). The failure was observed in the web members where the web started to have an overlapping condition with the chord. As the vertical reinforcing members had no tension anchorage, those members failed to reinforce the trusses at certain joint locations as Fig. 6(b) shows an example.

Figure 6: a) Second Reinforcement, b) Web Failure After Second Reinforcement

### *3.3.3 Vertical Web Member Type of Reinforcement II*

After observing the test-2 results, we found that the reinforcement at the weak points again it is not sufficient. Therefore, we removed two members which we added earlier. Then we came up with a different setup by adding one vertical like the previous one by replacing track (350T162-54) with stud(350S162-54) with top and bottom members, as shown in Fig. 7.

Figure 7: Third Reinforcement

### *3.3.4 Vertical Web Member Type of Reinforcement III*

After observing the third reinforcement results, we found that the reinforcement is not in the right position of weak points again it is not sufficient. The third reinforcement is changed the position to another flange of the web, as shown in Fig. 8.

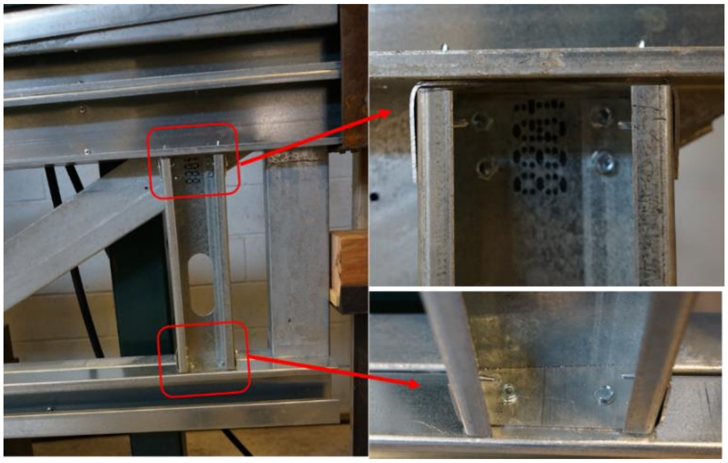

Figure 8: Final Reinforcement

### *3.4 Experimental Test Results*

A total of four trusses were investigated in this project, two 48 ft span, two 54 ft span trusses. For each truss, multiple tests were performed to develop optimal truss configurations. Some of the tests were stopped due to limitation of the displacement sensor and/or the cylinder travel distance, and their results were not included in the test result summary in Table 1.

Table 1: Experimental Results

| Test | Peak Reaction Force (lbs.) | Deflection at Peak Load (in.) |
|---|---|---|
| Test 1.1 | 2352 | 5.448 |
| Test 1.4 | 3676 | 5.585 |
| Test 2.1 | 2798 | 4.264 |
| Test 2.3 | 3786 | 6.300 |
| Test 3.1 | 2629 | 5.835 |
| Test 3.3 | 3257 | 5.454 |
| Test 4.1 | 2434 | 4.732 |
| Test 4.3 | 2924 | 5.96 |

## 4. Numerical study

Computational simulations allow for comprehensive assessments of truss performance, enabling researchers to simulate experimental tests and validate the results. This section focuses on discussing essential finite element modeling techniques for investigating the behavior and failure modes of the trusses under a uniform load, supported simply at both ends. The finite element models of full-scale trusses were initially developed in SolidWorks and subsequently imported into ABAQUS using the STEP File format. Further details of the developed finite element models are discussed in this section.

### *4.1 Finite Element Modeling*

In SolidWorks, we utilized the sketch module to design a C-section and the dimensions of the C-section members were selected from the AISI catalog, and the thickness was determined based on the results of the coupon test. Using the sheet metal module, we converted the C-section sketch into a C-section stud. Likewise, we created the web and ended members. By using the extruded cut tool, we removed the flanges and lip of the web members as shown in Fig. 9. Using the created parts by SolidWorks assembly module combined like experimental trusses as shown in Fig. 10. In the second step, we imported the created model into ABAQUS as a STEP file.

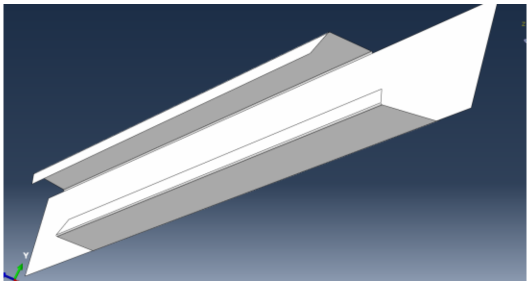

Figure 9: 3D Part Converted into 2D

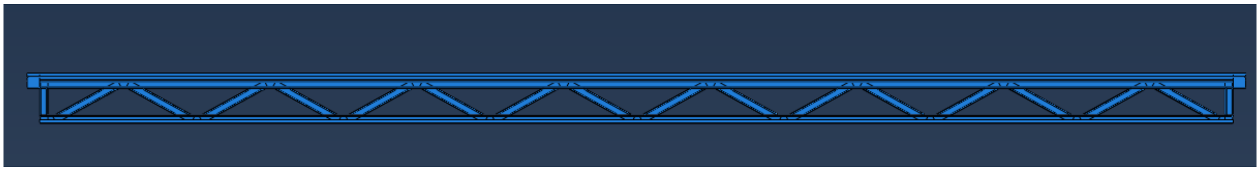

Figure 10: Assembly of Truss

All material properties of the CFS C-section were determined through coupon tests. Elastic and plastic material behaviors were assigned to all members. The elastic material behavior was modeled as isotropic, with a Young's modulus (E) of 29,500,000 psi and a Poisson's ratio (v) of 0.3. Concerning the plastic material properties, a total of 9 points, comprising the yield stress, yield strain, ultimate stress, and ultimate strain, were selected from the material properties. These points were then converted from engineering stress and engineering strain to true stress ($\sigma true$) and true strain ($\epsilon true$). The engineering stress and strain is an average of three coupon tests.

Before using Tie constraint, a mesh was created to generate a set of nodes at the screw connections for components such as the web-top chord, web-bottom chord, back-to-back section forming the chords, truss reinforcements, and top chord-end iron supports. A "Tie" constraint was then employed to connect the CFS members in the combinations. A sample is shown for the back-to-back node set to build chords in Fig. 11. It is crucial to note that the designation of members as either master or slave holds significant importance in FEA. Slave nodes "follow" the master nodes, and in these models, it is worth mentioning that a particular part or component can function as a master multiple times, but it can only serve as a slave once.

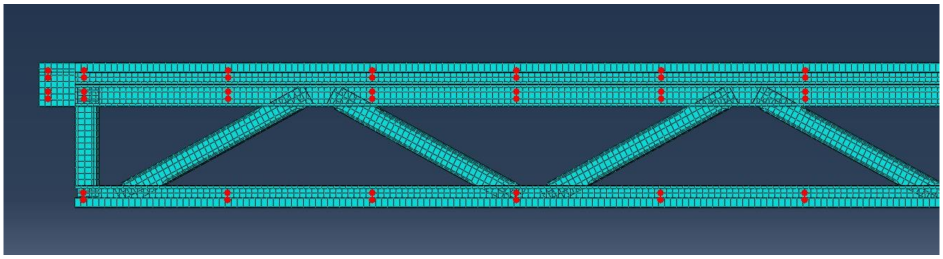

Figure 11: Sample of Node Set of the Back-to-Back Built in the Top and Bottom Chords

To restrict the truss from out-of-plane movement, a set of nodes was selected on each flange of the top chord and bottom chords, based on the experimental condition where wooden plates were available for lateral support as shown in Fig. 12. Similarly, surfaces were chosen on the iron supports at the ends of the top chord to apply a pinned condition effectively creating simple support. To prevent buckling, the remaining iron supports surfaces were selected to restrict movement in the z-direction, while the truss was positioned in the x and y plane.

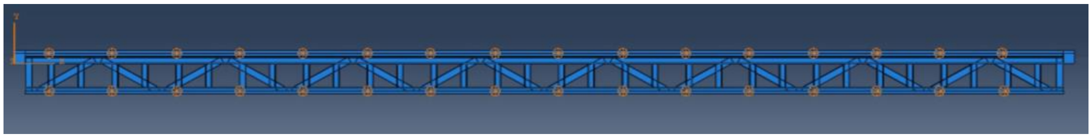

Figure 12: Restrict of the Top and Bottom Chord in Out-to Plane Moment and Displacement

A contact property was implemented between the surfaces of the flange of the C-section in the chords and the edges of the flanges of the web to prevent penetration through the chord members. The contact was set to exhibit a "frictionless tangent" behavior. This addition of the contact property also contributed to a reduction in the overall running time for the models.

By partitioning the top surface at both ends of the top chord by 6 in. on each side, the aim was to account for the reality that the load does not act uniformly on the iron support. Following the partitioning, the designated top surface was selected to apply a mechanical pressure load as shown in Fig. 13. The initial magnitude of the load was set as 1, but it varied depending on the failure and deflection shape, mimicking the behavior of a uniform load in the experimental testing.

Figure 13: Pressure Load on the Top chord

In FEA, the problem domain is discretized into a mesh comprising numerous tiny elements. Solving the partial differential equations (PDEs) for each mesh element and merging the results yields the solution for the entire domain. Mesh size significantly affects accuracy, emphasizing the importance of proper meshing. Our software offers various mesh shapes, and we employ a quad mesh of size 1 in. for simplicity and effectiveness. For 3D models, a tri mesh of size 0.1 in. is necessary, but it's more complex. Simulation time varies with mesh size. We initially tried a 1.5 in. mesh size, but issues arose at the web-flange junction of the C-section member. Reducing the mesh size to 0.1 in. for a 576 in. long-span truss increased simulation time due to the large number of components (60). Therefore, we opted for a 1 in. mesh size to balance accuracy and computational efficiency.

### *4.2 Observations from Simulation*

Finite element modeling results are compared with experimental test results in terms of deformation and stiffness. In truss design, two critical criteria are considered: maximum load-bearing capacity and deflection of the trusses. Long-span truss deflection significantly affects overall structural behavior before reaching peak load, so focus is primarily on deflection. Using a linear graph showing the relationship between vertical displacement at the truss center and reaction force, we determined truss stiffness in the both experimentally and numerically. The graph plots vertical displacement against reaction force.

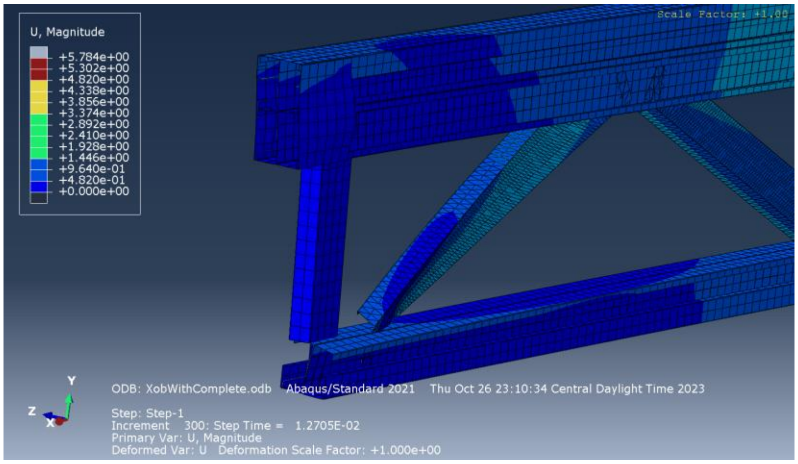

Figure 14: Failure of the Web Member

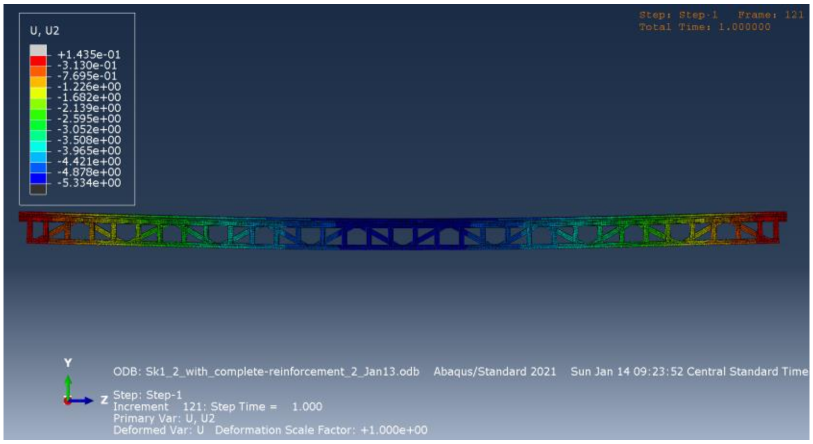

Figure 15: Truss Bending

## 5. Results

To compare experimental with numerical analysis, we examine the initial linear displacement versus reaction force graphs. From these graphs, we determine the stiffness, and the average values are compared in Table 2.

Table 2: Comparing Numerical results with Experimental Results Based on Stiffness

| Truss Length (ft) | Experimental Stiffness (lb/in.) | Numerical Stiffness (lb/in.) |
|---|---|---|
| 48 | 760.53 | 716.2 |
| 54 | 552.86 | 610.06 |

The comparison of experimental tests with numerical analysis was done using the initial linear displacement versus reaction force graph, as shown in Fig. 16 to Fig. 19 where experimental curves of multiple tests on each truss are presenented along with the finite element results. It can be concluded that the finite element models had a good agreement with the test results with regard to the initial stiffness which is the most significant of long span trusses for structural design purposes.

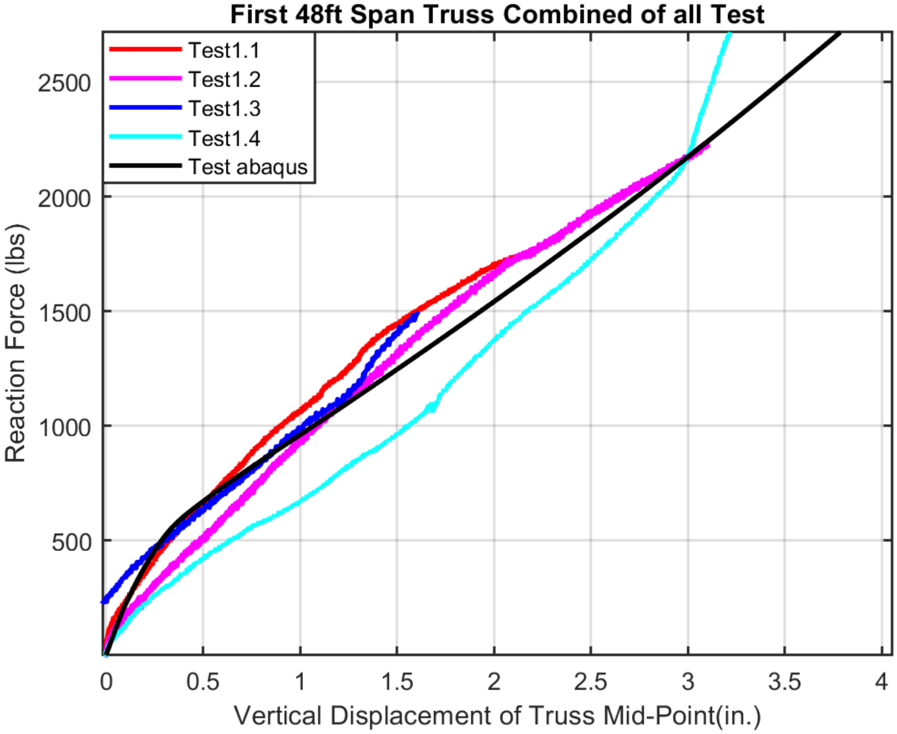

Figure 16: The comparison of experimental tests with numerical analysis of first 48ft span truss

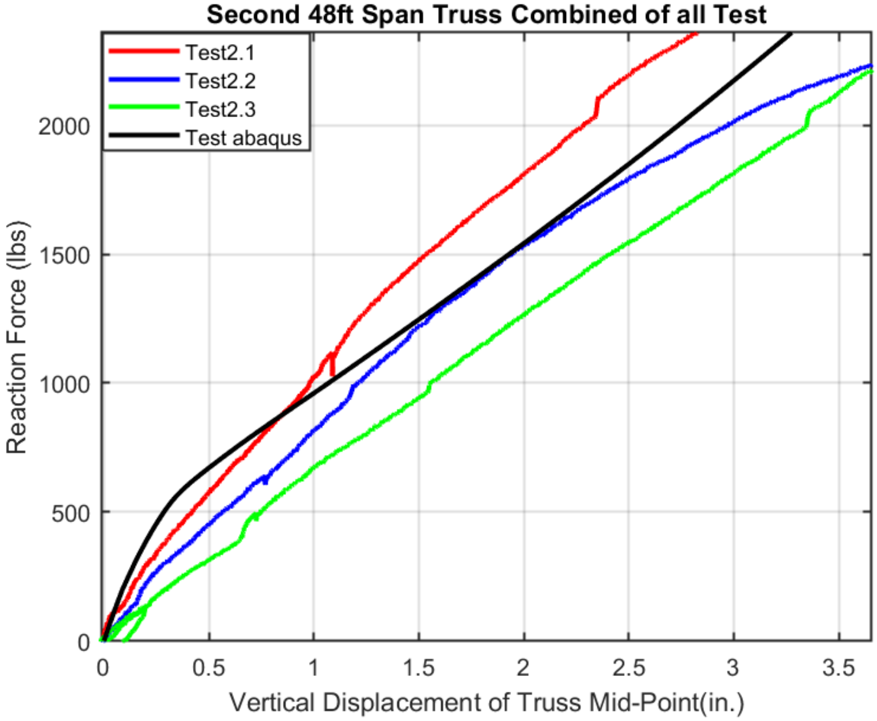

Figure 17: The comparison of experimental tests with numerical analysis of second 48ft span truss

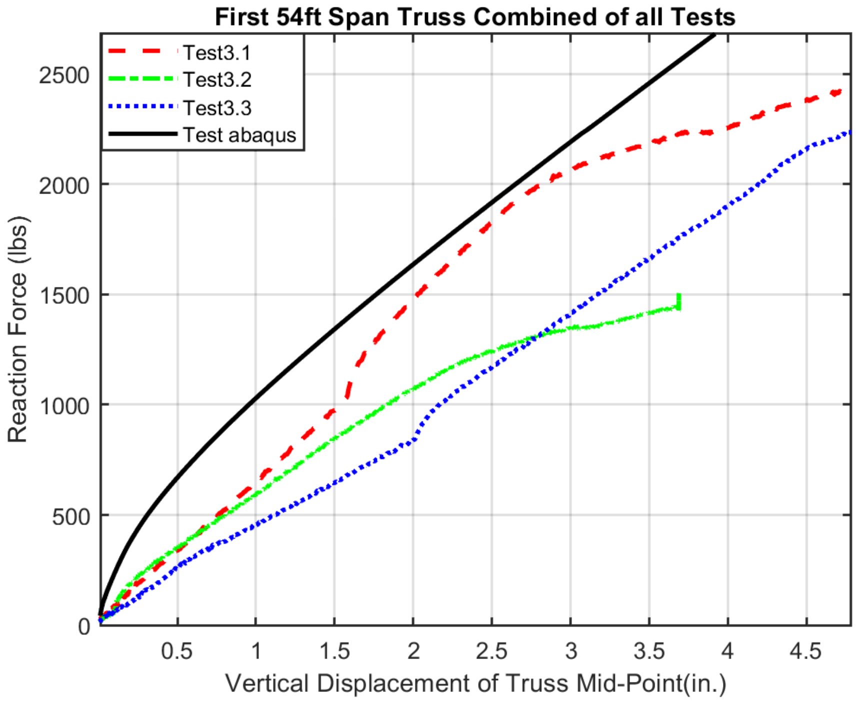

Figure 18: The comparison of experimental tests with numerical analysis of first 54ft span truss

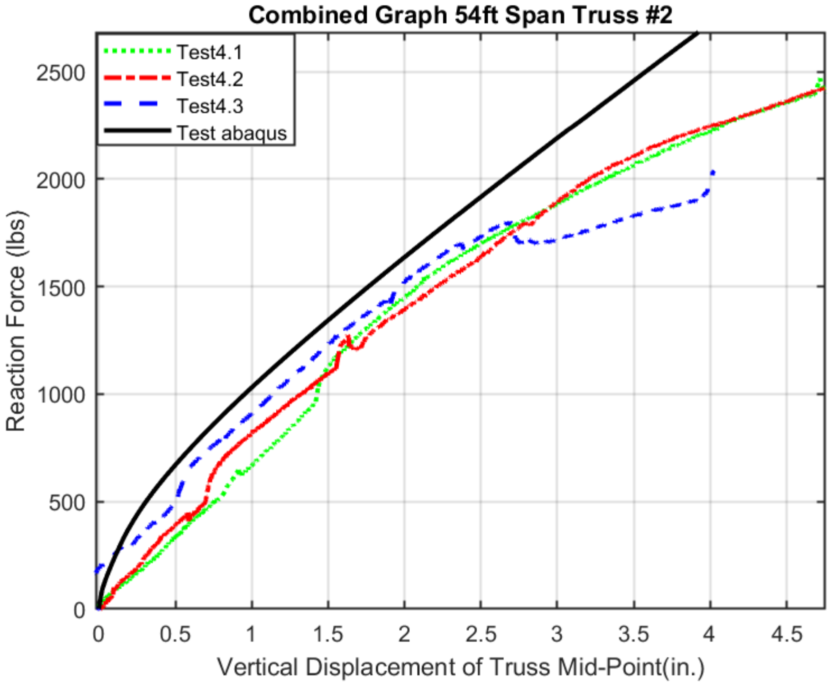

Figure 19: The comparison of experimental tests with numerical analysis of second 54ft span truss

## 6. Conclusion

The experimental testing and numerical simulations have conclusively demonstrated that the original design of the trusses experienced failures in the web members. Subsequently, enhancements were made to reinforce both the truss webs and the web-to-chord connections, resulting in increased strength and stiffness. The improved long-span cold-formed steel trusses show commendable performance, demonstrating higher load bearing capacity and a more favorable failure mode than the initial design. The test and simulation data serve as valuable references for the design and construction of non-proprietary long-span trusses by using standard cold-formed steel ‘C’ members as per the American Iron and Steel Institute/Steel Framing Industry Association /Steel Stud Manufacturers Association for use in building floors and roofs. These test results can be employed as a benchmark for future research and development of those long-span trusses in flooring and roofing systems.

## References

AISI S100 (2016). North American Specification for the Design of Cold-Formed Steel Structural Members, 2012 Edition. American Iron and Steel Institute, Washington DC.

ASTM A370 (2010). Standard Test Methods and Definitions for Mechanical Testing of Steel Products. American Society for Testing and Materials, Conshohocken, PA.

AISI S201 (2012). North American Standard for Cold-Formed Steel Framing – General Provisions, 2012 Edition. American Iron and Steel Institute, Washington DC.

Xu, L., Min, H., & Schuster, R. M. (2000). Optimum design of Cold-Formed steel residential roof trusses. International Specialty Conference on Cold-Formed Steel Structures: Recent Research and Developments in Cold-Formed Steel Design and Construction.

Cold-Formed Steel Trusses: Design, Performance, and Advantages Cold-Formed Steel Framing Resource Center for Building Professionals. (n.d.). Retrieved October 27, 2023.

BXUV.H524 - Fire-resistance Ratings - ANSI_UL 263 _ 1-11-2021. (n.d.).

The Only Cold-Formed Steel Truss Designed Specifically for Flat Roof and Floor Applications ADVANT Bar Joist Replacement Why ADVANT instead of Bar Joist? (n.d.). www.advantsteel.com

Wolfe, R. W., Stahl, D., & Cramer, S. (1996). Experimental Assessment of Wood Trusses with Square-End Webs. Experimental Assessment of Wood Trusses with Square-End Webs.

Shotton, E. (2015). THE EVOLUTION OF THE IRON TRUSS IN THE WORK OF JOHN RENNIE.

Dara, M. L. (2015). Direct Strength Method for Web Crippling of Cold-Formed Steel C and Z Sections subjected to Interior One Flange Loading and End One Flange Loading. Truss score material and science. (n.d.). Retrieved November 2, 2023.